Arabian Journal of Geosciences (2022) 15: 939
https://doi.org/10.1007/s12517-022-10239-7

ORIGINAL PAPER

Pixel-based classification techniques for automated shoreline extraction on open sandy coast using different optical satellite images

Chenthamil Selvan Sekar[1] · Roop Singh Kankara[1] · Prabhu Kalaivanan[1]

Received: 8 September 2021 / Accepted: 28 April 2022 / Published online: 6 May 2022

Abstract
The coastline and their landscapes are at constant risk due to various natural hazards. Shoreline monitoring and mapping are essential for proper coastal zone planning, development, management, and divisive conservation schemes. Digitizing shoreline position manually is a time-consuming process, and manual errors are a concerning factor. The present study proposed a pixel-based classification technique on optical images to extract the proxy-based (wet/dry) shorelines on an open sandy coast. A composite technique, which is a combination of band ratio (green/mid-infrared band) and histogram thresholding (near-infrared band), was applied on Landsat-7 (ETM + — Enhanced Thematic Mapper Plus) image. An unsupervised classification (ISODATA — Iterative Self-Organizing Data Analysis Technique) technique using multi-spectral (green, red and near-infrared) bands were applied to the Resourcesat-2 (LISS-IV — Linear Imaging Self-Scanning Sensor) image. Pre-processing techniques such as geometric correction and noises from the images were reduced, and then the proposed techniques were implemented to extract the shoreline position from the raster images automatically. The robustness and accuracy of the automated shoreline are compared and validated with the in situ field measured data. The comparison shows that 87.5% of the transects fall less than 2 m accuracy (less than half of a pixel of LISS IV — 5.8 m), whereas K-mean, NDWI, and maximum likelihood methods show the accuracy of 83%, 79%, and 75%, respectively. Compared to other remote sensing techniques, the shoreline positions extracted from the ISODATA techniques produce a consistent result with open sandy coast. This study provides a comprehensive, reliable, and standard, repeatable automatic method for extracting the shoreline position from optical satellite images for a similar type of coastal landscape, which ultimately reduces the time duration and leads to rapid monitoring of the coast.

Keywords Shoreline extraction · Remote sensing · Histogram thresholding · Band ratio · Unsupervised classification

Introduction

Beach erosion is one of the persistent problems along many shores of the world. Coastal erosion is considered a slow and continuous natural phenomenon occurring in day-to-day life. According to coastal researchers, the action of waves, wind, tide, near-shore currents and artificial structures such as groins, seawalls and breakwaters are significant factors for coastal erosion. About 20% of the world population lives within 25 km from the coastline and 40% within 100 km from the coastal stretch (Hinkel et al. 2014). Populations along the coast continue to increase, and thereby the infrastructures along the coast are endangered by coastal erosion. Natural and anthropogenic activities often exacerbate the shoreline change and increase the risk factors along the coast. The constant change in shoreline position is considered as one of the major concerns for coastal developmental activities such as ports, fishing harbour jetties and embankment facilities. Therefore, it is necessary to understand the past and present shoreline positions. The change in shoreline position over time is of elemental importance to coastal scientists, engineers, and managers for coastal management and engineering design for 13 coastal development. Therefore,

Responsible Editor: Biswajeet Pradhan

✉ Chenthamil Selvan Sekar
tamil@nccr.gov.in

Roop Singh Kankara
kankara@nccr.gov.in

Prabhu Kalaivanan
prabhu@nccr.gov.in

[1] National Centre for Coastal Research (NCCR), MoES, Chennai, India 600100

precise shoreline information on past and present shoreline trends is required for designing the coastal protection, structure calibration/verification of numerical models, assessment of sea-level rise, preparation of hazard zones, formulation of policies, the regulation of coastal developmental activities, etc.

Shoreline mapping and change analysis is considered as one of the major natural hazards where more focus needs to be emphasized by coastal researchers. Past shoreline, the position is considered as the major tool to understand the significance of sea-level rise and other natural hazard futuristic prediction. There are many methods employed by coastal researchers which include the basic conventional field survey method, use of topographic maps, aerial photographs, and the latest remote sensing data with medium to high spatial resolution. Shoreline detection using multi-spectral satellite images has become a more common dataset due to its availability, wide spatial coverage, time interval and, more importantly, availability of high spatial resolution images. Landsat (TM — Thematic Mapper, ETM +), SPOT, Resourcesat-1 (LISS-III), etc. are categorized under medium spatial resolution images, which are freely available to download, by the concerned authorities. High-resolution images include satellites such as Resourcesat-2 (LISS-IV), Cartosat-1, 2 and 3 (Panchromatic), IKONOS, Worldview and QuickBird. Remote sensing data in the GIS environment have been extensively used for shoreline change studies (Nayak 2002; Zuzek et al. 2002; Thieler et al. 2009). Remote sensing data provides a rapid, repetitive, synoptic temporal coverage. Conventional ground survey method such as differential Global Positioning System (DGPS) ARCPAD survey is considered to provide an absolute shoreline position. However, labour, expensive and time consuming are some of the significant problems (Mitra et al., 2017). In remote sensing data, choosing the best image is the most significant challenge for the coastal researcher. Each satellite data has its uniqueness in terms of spatial resolution, spectral band, temporal repeatability, sensor characteristics, etc. Therefore, selecting the best satellite data for any particular study is of prime importance of shoreline extraction.

Satellite data may be of different forms, such as multi-spectral images, hyperspectral images, airborne Light Detection and Ranging (LiDAR) and microwave images (Boak and Turner 2005). According to Boak and Turner (2005), multi-spectral satellite images are considered the best data product for shoreline extraction due to the availability of image repeatability periods. Optical satellite data provides a wide range of information and easy-to-interpret features. According to Moore (2000), TM (Thematic Mapper) and ETM + (Enhanced Thematic Mapper Plus) provide ground information in different bandwidths. Alesheikh et al. (2007) used TM and ETM + data for shoreline detection along Urmia Lake. Chang and Brumbley (1999) studied the shoreline change using SPOT multi-spectral satellite image. Yasir et al. (2020) used multi-spectral Landsat (ETM + and OLI — Operational Land Imager) image for 19 years along the Qingdao coast of east China. They applied the canny edge detector method to extract the shoreline positions in the GIS environment. Biswajeet et al. (2018) studied the coastline dynamic and change study using synthetic aperture radar (SAR) images such as Radarsat-1 and 2. Filtering techniques and image enhancement methods were adopted on the SAR images to reduce the uncertainties in the images, which are being used. Similarly, A'Kif et al. (2011) used Radarsat-1 (SAR) image for shoreline extraction using semi-automated method. Here, the enhanced filtering technique was adopted for shoreline extraction. Abdelhady et al. (2022) developed a new water body and land separation index. They named the index as Direct Difference Water Index (DDWI). Some of the recent satellite data such as Planetscope, RapidEye, Sentinel 2 and Landsat 8 were used to extract the shoreline boundary automatically. These extracted shorelines are then validated with beach survey data using a novel backpack-based LiDAR system. High-resolution satellite such as IKONOS satellite image has been used to extract the shoreline position using the semi-automated method (Di et al. 2003). Similarly, Sekovski et al. (2014) extracted the shoreline position using WorldView-2 multi-spectral image. They integrated both supervised and unsupervised classification techniques in his research work.

Landsat Thematic Mapper (TM) band 4 (infrared-IR) was used to demarcate the land/water boundary (Ellis et al. 1991; Tao et al. 1993; Tittley et al. 1994). Krishna et al. (2005) used band 5 of Landsat image to automatically identify the land, water and transition zone using a simple density slice (threshold techniques). The infrared band of the Landsat image shows strong absorption of water and strong reflectance of vegetation and other land features. Hence, the near-infrared band gives an ideal combination for demarcating the land and water boundary (DeWitt and Weiwen Feng, 2002). Krishna et al. (2005) applied the Iterative Self-Organizing Data Analysis Technique (ISODATA) clustering method on Linear Imaging Self-Scanning Sensor (LISS-III) Bands 2, 3 and 4 for land/water boundary discrimination for Sagar Island. They even correlated the principal components analysis (PCA) method on all three Indian Remote Sensing (IRS/LISS-III) spectral bands to determine the best land/water boundary combinations. Red (band-3) and near-infrared (band-4) of LISS-III data were applied for the NDVI (Normalized Difference Vegetation Index) analysis (Krishna et al., 2005). Band 3 shows a low reflectance value, whereas Band 4 shows higher reflectance values of healthy vegetation. According to Aedla et al. (2015), in near-infrared (NIR) wavelength, the vegetation or soil appears brighter due to its strong reflectance. Water features appear darker due to the strong absorption by the particular wavelength. Shoreline

positions can be mapped using pixel-based classification techniques or object-based classification techniques. Unsupervised classification (ISODATA) methods were applied to Thematic Mapper (TM) to map the water bodies with more than 95% accuracy (Kingsford et al. 1997; Frazier and Page 2000). Mitra et al. (2017) have used different methods such as NDVI, Water Index, Complex band ratio techniques, thresholding and ISH transformation techniques to extract the shoreline position and provided the best combination of automated techniques. Chen Chao et al. (2019) applied the tasseled cap transformation (TCT) method to extract the coastline position from Landsat-8 (OLI) images. They applied the TCT method along the Yangtze River Estuary, located in the eastern region of China. According to Chen Chao et al. (2019), coastline position was extracted by applying four different steps such as radiometric correction, modelling with wetness and greenness, then coordinates geometry and finally accuracy assessment. Song et al. (2019) have emphasized the pixel-based classification technique for extracting the shoreline position. They experimented with a semi-global subpixel shoreline localization method (SGSSL) using Landsat-8 (OLI) satellite image to extract the shoreline position. Apostolopoulos and Nikolakopoulos (2021) have published a review article on different remote sensing methods for shoreline extraction both automatically and manually. The review article highlights the software's data and even data used during the past 20 years.

The National Centre for Coastal Research (NCCR) has studied the shoreline change for the Indian coast using Indian Remote Sensing (IRS) satellite images and Landsat images as the primary data source. Many shoreline change works were carried out by NCCR using remote sensing applications in the GIS platform. NCCR, under the Ministry of Earth Sciences (MoES), has published an atlas entitled "National Assessment of Shoreline changes along Indian Coast: Status report for 26 years (1990–2016)" (Kankara et al. 2018). Semi-automated (automatic and manual digitization) shoreline extraction method was performed to evaluate the shoreline change rate along the Indian coast. The present study is a part of an ongoing research program under the "Coastal Processes and Shoreline Management" project. A new methodology (automated shoreline extraction) was proposed to implement for the extraction of shorelines.

Coastal researchers have used different techniques to extract the shoreline based on the area of interest and applicability. Each method in different studies provides different accuracy levels. Hence, it depends on the researcher to provide suitable methods for the corresponding study. There is a need for a proper and efficient method to calculate the shoreline change rate accurately. Hence, the study's main aim is to develop a proxy-based (wet-dry line) approach for the automatic shoreline extraction from different optical satellite images using digital image processing techniques. In this process, two different methods were adopted to extract the shoreline position. One is the composite technique (combination of both band ratio and histogram thresholding method) for medium spatial-resolution satellite images (Landsat-ETM +) and the second method is the unsupervised classification (ISODATA) technique for fine spatial-resolution images (Resourcesat-2, LISS-IV). Finally, the extracted shoreline position is validated with the in situ measured shoreline from the field. There are very few or no studies undertaken on LISS-IV images for shoreline extraction. Shoreline validation and accuracy assessment were carried out by quantitative evaluation method. In the quantitative method, validation of the shoreline is carried out by comparing the field-measured shoreline position with the extracted shoreline from the fixed baseline (reference line). Different image processing techniques such as normalized difference water index (NDWI), supervised classification (maximum likelihood — ML) method and K-mean method were compared with the ISODATA method. Even though each method is within the pixel limit, the ISODATA method shows more accuracy when compared with other methods. The manual digitization of shoreline position is a time- and cost-consuming process, which can be reduced significantly by an automated method. The present study provides a comprehensive, reliable and repetitive method for shoreline extraction from optical satellite images (ETM + and LISS-IV sensors) along the sandy coast and minimizes the time duration and human errors.

Dataset used

Two different optical satellite data have been widely used for this study. One is a medium-resolution satellite (Landsat-7, ETM + sensor) downloaded from US Geological Survey (USGS) web portal earth explorer https://earthexplorer.usgs.gov/ and the other is the high-resolution satellite image (Resourcesat-2 (LISS-IV sensor) procured from the National Remote Sensing Center (NRSC). Landsat-7 is equipped with eight spectral bands. Indian Remote Sensing satellite such as Resourcesat-2 (LISS-IV sensor) has three (green, red and NIR) different spectral bands. Details of each band in Landsat-7 and Resourcesat-2 are shown in Table 1. According to Parker and Wolff (1965), each wavelength in the electromagnetic spectrum has a unique response to ground features. Each spectral band in the images is designated with a different rationale to record the ground features. Similarly, various landforms such as land and water were demarcated from these spectral bands automatically by image processing techniques. In a medium-resolution image, grey bands (green, near-infrared and mid-infrared) were applied. Instead, in fine-resolution, a multi-spectral image (green, red and near-infrared) was used for extracting the shoreline position. For

Table 1 Details of Landsat-7 and Resourcesat-2 satellite data with its spectral bands

Band	Spectral bands name	Wavelength (μ)	Spatial resolution (m)	Sensor	Acquisition period	Source
Landsat-7 image						
1	Blue	0.450–0.515	30	ETM +	22 March 2013	USGS
2	Green	0.525–0.605	30			
3	Red	0.630–0.690	30			
4	Near-Infrared	0.760–0.900	30			
5	Mid- Infrared	1.550–1.750	30			
6	Thermal-Infrared	10.40–12.5	60			
7	Long- Infrared	2.080–2.35	30			
8	Panchromatic	0.52–0.92	15			
Resourcesat-2 image						
1	Green	0.52–0.59	5.8	LISS-IV	06 April 2013	NRSC
2	Red	0.62–0.68	5.8			
3	Near-Infrared	0.77–0.86	5.8			

different image processing techniques, ERDAS IMAGINE-2014 V and ENVI-5.3 V software were used. Histogram thresholding and band ratio techniques were carried out by ENVI-5.3 V. Similarly, ERDAS IMAGINE-2014 V software was used for other processing techniques such as ISODATA, NDWI, K-mean and maximum likelihood methods. Arc-GIS 10.3 V software was used for shoreline smoothing, conversion and validation.

Shoreline indicators

Before getting into shoreline extraction, it is necessary to define the shoreline proxies in satellite images to monitor the coast continuously. The coastal region provides different geomorphologic conditions, tidal variations, changes in near-shore bathymetry, various vegetative covers types, etc. As the shoreline is highly dynamic, different proxies can be interpreted from satellite images. Comparing the shoreline positions with the real shoreline position is a difficult task (Toure et al. 2019). This is mainly due to different morphological settings where one indicator cannot be used to determine the shoreline with different signatures. Some of the proxies of shoreline used by different coastal researchers are high tide line (Fisher and Overton 1994; Stockdon et al. 2002), high water line (Shalowitz 1964; Fenster and Dolan 1999), wet-dry line (Overton et al. 1999; Moore et al. 2006), vegetation line (Hwang 1981; Hoeke et al. 2001), dune line (Stafford and Langfelder 1971; Moore and Griggs 2002), toe or berm of the beach (Norcross et al. 2002), cliff base or top (Hapke and Reid 2007), mean high water (MHW) line (Morton et al. 2004), low water line (Fletcher et al. 2003), etc. Hence, choosing the best available proxy for shoreline extraction using a satellite image for the particular study becomes necessary. Wet/dry shoreline proxy was applied for shoreline extraction using multi-spectral satellite images (Sekovski et al. 2014). The spectral signatures of sandy shore were interpreted along the coastal region of Ravenna Province of Italy. Tarmizi et al. (2014) used vegetation line as shoreline indicator. The spectral signature of vegetation and sandy shore can be distinguished and interpreted easily by different pixel values. Moreover, the vegetation line is towards the inland and makes the shoreline proxy simpler when compared to other proxies. Even Rogers et al. (2021) used the vegetation line as a proxy for shoreline extraction automatically. They developed a VEdge Detector method to extract the shoreline. Luijendijk et al. (2018) fixed sandy beach as one of the indicators for shoreline position. They assessed the shoreline change on global scale using pixel-based supervised classification technique on different multi-spectral images. Mentaschi et al. (2018) interpreted the shoreline positions using different shoreline proxies such as rocky coast, sandy coast and gravel beaches on multi-spectral satellite images. Based on the interpreter's knowledge, the precision of the outcome may vary from person to person. Even the same interpreter can provide several outputs using different shoreline proxies from the same satellite image. Therefore, in the present study, the wet/dry line, which can be clearly interpreted from the satellite images, was used as a proxy to extract the shoreline position automatically on sandy shore. This wet/dry line proxy is easy to interpret from satellite images and minimizes the interpretation error.

The automated shoreline extraction method was applied to the open Chennai coast, situated at the south-eastern corner of the Indian peninsular. It covers about 6 km of coastal length from the Coovum River on the north to the Adyar River on the south (Fig. 1). The coastal length is almost linear and shows a north–south orientation. Chennai coast is one of the densely populated urbanized cities on the east

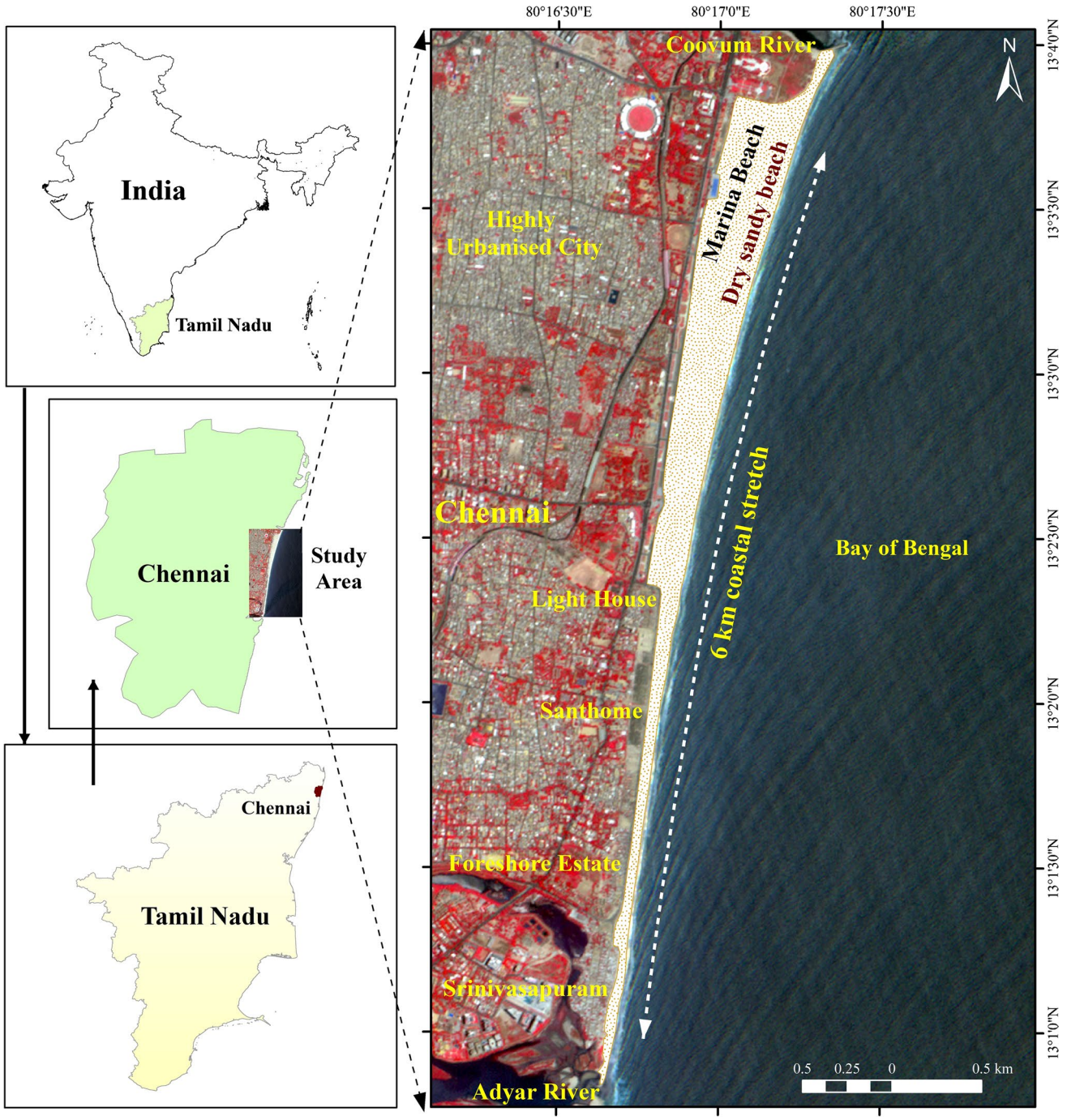

Fig. 1 Study area location map

coast of India. Marina beach, Lighthouse and Foreshore Estate are some of the prominent places occupying the study area. Some of the significant land covers in the study area are wide-open sandy beaches, vegetation, urbanized colonies, road network, rivers, etc. The presence of different landforms and wide-open sandy beaches makes the Chennai coast ideal for carrying out the automated proxy-based shoreline extraction to better interpret an urbanized coast.

Proposed methodology

The methodology proposed in the present study is shown in the flow diagram (Fig. 2a and b). Two different methodologies have been proposed in the current study. One is for medium spatial-resolution image (Landsat-7) and the second is for high spatial-resolution image (Resourcesat-2).

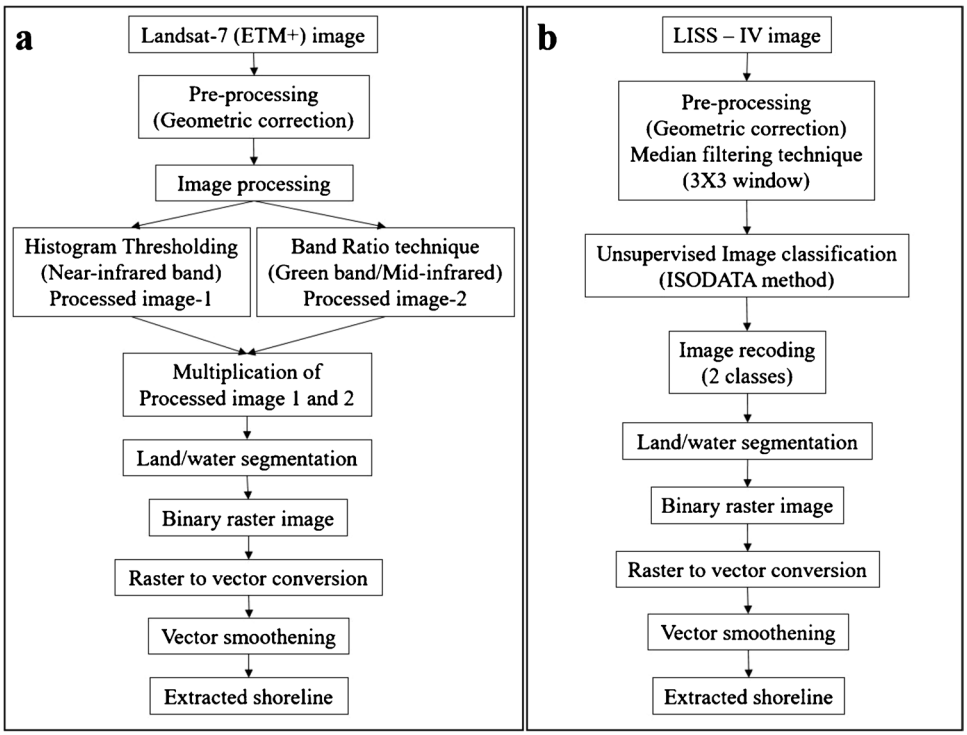

Fig. 2 **a** Flow chart representing the step-wise procedure for automated shoreline extraction from Landsat-7 satellite image; **b** flow chart representing the step-wise procedure for automated shoreline extraction from Resourcesat-2 satellite image

Each methodology has different step-wise procedures that need to be followed.

The proposed automatic shoreline extraction method for the Landsat image is obtained from the following steps:

- Image pre-processing (geometric correction)
- Histogram thresholding (near-infrared band) — processed image-1
- Composite band ratio technique (green/mid-infrared band) — processed image-2
- Multiplication of processed image 1 and 2
- Land/water segmentation (binary image)
- Raster to vector conversion
- Smoothing application in GIS environment
- Shoreline extraction

Similarly, the proposed steps-wise procedures for Resourcesat image to extract the shoreline positions are.

- Image pre-processing (geometric correction and median filtering)
- Unsupervised classification technique (ISODATA)
- Image re-coding
- Raster to vector, conversion
- Smoothing application in GIS environment
- Shoreline extraction
- Field validation (accuracy assessment)

Initially, the pre-processing technique was applied on the satellite image to minimize the error in the image while calculating the shoreline position. Next, the global histogram thresholding method was applied on Landsat-7 (band-4 — Near-infrared band) to segregate the image in to binary image (raster image). On the other hand, band ratio technique was adopted for band 2 (green) and band 5 (mid-infrared) of Landsat image. Then, the multiplication of images obtained from histogram thresholding and band ratio techniques was carried out to generate a composite binary image. This binary image is then segregated into a land/water boundary by applying the conversion method (raster to vector) in ArcGIS environment. Smoothing technique was applied on the vector file to extract the final shoreline position.

Similarly, the pre-processing technique was applied on the satellite image and then the median filtering technique was performed on multi-spectral bands of the Resourcesat-2 (LISS-IV) image. The combinations of bands used in the LISS-IV analysis are green, red and near-infrared. Then, the ISODATA technique was applied to the multi-spectral filtered image. Initially, 15 classes were generated through the ISODATA technique and then re-coded to land, water and unclassified-mixed pixels. Now, this raster image is classified into land and water pixels based on the shoreline proxy (wet/dry line). Once the image is created, the next step is to convert the raster image into a vector format (shapefile). Finally, the smoothening technique was performed on this shapefile using ArcGIS 10.3 V software to obtain a final shoreline position.

The methods used in this study have their uniqueness in extracting the shoreline positions. Various image-processing

techniques such as NDWI, supervised (maximum likelihood) and unsupervised (K-mean) classification techniques were analyzed separately to the image. Even though all the techniques created an output image, the accuracy level varied largely. However, the unsupervised technique (ISODATA) outcome provided a promising result, discussed in the proceeding sessions. Similarly, a composite technique, a combination of thresholding and band ratio, was applied to the Landsat image, and the outcome provided a very encouraging result.

Geometric correction

Image correction is the preliminary step in the pre-processing technique. The satellite image should be brought into a common projection system so that the error in the image while calculating the shoreline position can be minimized. All the satellite images were rectified using field-collected ground control points (GCPs) using a handheld GPS (Global Positioning System). GCPs were collected from concrete landmarks such as road-rail intersections and two road intersections points ERDAS IMAGINE 2014 software was used to rectify the satellite image. Second-order polynomial method was employed (minimum of 6 GCPs required) for rectification (projection: UTM, Datum: WGS-84). In this study, a total of 16 GCPs were evenly distributed throughout the image. The root mean square error (RMSE) value of all the satellite images was maintained within one pixel level.

Band threshold approach:

Histogram thresholding is applied to segregate different grey bands into several different classes. Histogram thresholding method is considered as one of the easiest methods for image separation into different classes. Otsu's (1979) method was considered as simplest and a widely used thresholding method to segregate the grey band into a binary raster image. Otsu (1979) has explained the selection of optimal threshold values by the discriminant criterion. The Otsu method automatically divides the grey band by fixing the threshold value (transition value) into binary image. Fixing the transition value automatically has its own merits and de-merits. Thresholding value in an image can be obtained either by the local adoptive method or through the trial-and-error (T&E) method (Liu and Jezek, 2004). According to Liu and Jezek (2004) the trial-and-error method is widely used for shoreline extraction. They used the grey band for histogram thresholding. Jishuang and Chao (2002) proposed a multi-threshold based morphological approach. They divided the image into intracontinent, exterior sea and along the coastal region. The thresholding values were achieved by the segmentation of land, water and transition zone by altering the contrastive histogram (Krishna et al., 2005). Toure et al. (2019) suggested that the thresholding methods are mainly developed to segment the greyscale images. However, this method is insufficient for multi-spectral (MS) and hyper-spectral (HS) images due to the complexity of obtaining the information without data loss. Aedla et al. (2015) used adaptive thresholding techniques to extract the shoreline from Indian Remote Sensing Satellite (LISS-III). According to Alesheikh et al. (2007), the thresholding method will not provide an accurate shoreline position due to the selection of threshold values in the transition zone. In the present study, the single-band thresholding method was adopted on Landsat image (band-4, near-infrared band) to segregate the image into binary class. Many experiments were undertaken with different transition zone (T) to select the best transition zone (T). Band 4 is considered the best band for discriminating against the land and water pixels separately. The near-infrared (NIR) band, the water region appears to be dark in colour when compared to vegetation or sandy area. Due to the strong absorbance of water in NIR band, it appears as dark grey colour. The sandy region or vegetation has high reflectance in NIR band and hence appears lighter grey in colour. Figure 3apresents the histogram of the near-infrared band, which exhibits two distinct peaks and a valley. These

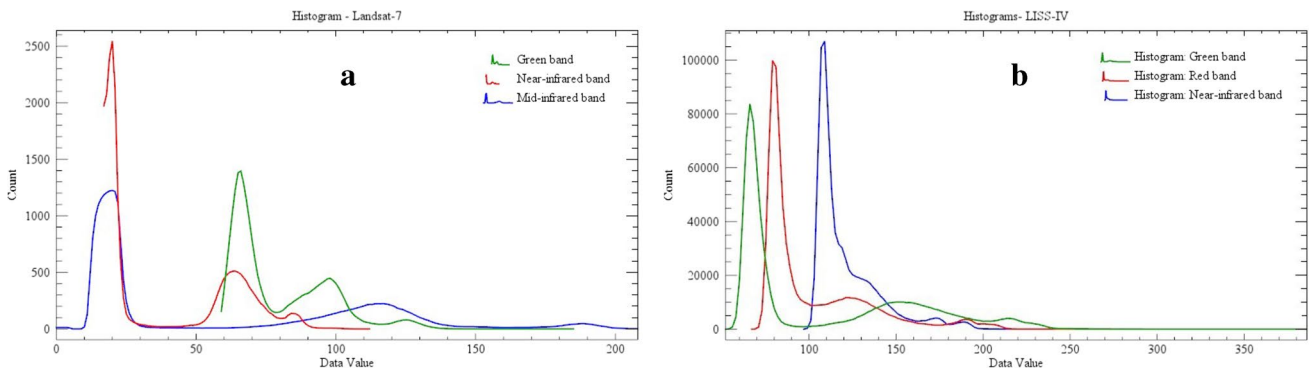

Fig. 3 **a** Histogram of green, near-infrared and mid-infrared band of Landsat-7 image; **b** histogram of multi-spectral Resourcesat-2 image

peaks perhaps represent a different spectral signature of the ground feature. The highest peak represents water pixels. In contrast, the small peak on the right side of the histogram represents the land pixels. A wide range of distribution was seen for the land cover features.

Band ratio technique

The band ratio technique adopts two different spectral bands. Each spectral band in any satellite has its own signature of ground features. Each band is designed with different applications of the earth's surface. Band ratio techniques are calculated by dividing one spectral band's pixels (DN values) by the corresponding pixels (DN values) in another band. The band ratio method has a significant advantage when compared with the other method. According to Tran and Trinh (2009), the variation in the pixel values of a single spectral band can be minimized by the ratio between two bands. Xu (2006) used the modified Normalized Difference Water Index (MNDWI) to demarcate the land–water boundary. Al Mansoori et al. (2016) adopted the spectral band ratios approach to classify the land–water boundary. He has explained two normalized difference indices. One is NDVI (normalized difference vegetation index), and the other is NDWI.

In the present study, the band ratio technique was applied to the Landsat-7 image. Two bands in Landsat-7 (band 2 and band 5) were chosen for the ratioing technique. Band 2 and band 5 are susceptible to turbidity differences in the water body. This will provide insight information on slight differences in the water body of the study area. According to Kelley et al. (1998), band 5 (mid-infrared) is considered the best band for extracting the land–water boundary. In band 5, the water bodies appear dark and separate themselves from other land covers such as barren lands, croplands and grasslands, which appear in a lighter tone. Therefore, ratioing the bands 2 and 5 will provide an image with two different land covers.

ISODATA — unsupervised classification techniques

The iterative self-organizing data analysis (ISODATA) method is purely a pixel-based unsupervised classification method. According to Toure et al. (2019), the ISODATA method is an enhanced version of the K-means classification method. The algorithm used in the ISODATA method is almost the same as that used in the K-mean method. However, the ISODATA method will statistically determine the pixel groups after each iteration run, which is an added advantage in this method (Pais-Barbosa et al. 2011). There are different steps such as initial unsupervised classification, masking the problem class, second-stage classification of problem class, recoding output from second-stage classification and finally merger of classification results to obtain the accurate results from the ISODATA method (Lillesand et al. 2015). This method can be applied to both panchromatic images (single band) or even in multi-spectral images. In the ISODATA method, the user itself can set the parameters needed for the analysis according to the area of interest to be analyzed. The class numbers are fixed based on the land cover of the study area analyzed. The classes should be set in a higher range for the coastal region due to the different land features (Liu et al. 2011). Braud and Feng (1998) have said that the ISODATA method is very much applicable for complex region studies. Krishna et al. (2005) suggested multi-spectral images (green, red and infrared) for land/water identification. The ISODATA method was adopted in our recent study to classify the land and water separately.

Shoreline change result

The single-band (greyscale) method was adapted to the Landsat-7 image. However, multi-spectral images were used in the Resourcesat-2 image. The step-wise procedure for shoreline extraction with Landsat and Resourcesat-2 image was discussed below in detail.

Shoreline extraction using Landsat-7 image

In a Landsat image, a composite technique was applied to extract the final shoreline position. It is a combination of both histogram and band ratio techniques. In the first step, the global histogram thresholding method was applied to the grey image (band 5). The thresholding method is used to separate an image into two different segments. In an image processing technique, an image's histogram refers typically to a histogram of the pixel intensity values. The intensity value defines the segments. The histogram of band 4 clearly shows two different peaks. Figure 3a shows the histogram of band 4 with two distinct peaks. Histogram thresholding of TM band 4 depicts two different peaks. These peaks represent the different spectral signatures of the ground feature. This is due to the high reflectance of vegetation and soil and low reflectance of the water body. The layers between the peaks are the transition zone (T), which is affected by mixed pixels between two different features.

Due to these mixed pixels, identifying the appropriate value becomes very difficult from histogram thresholding. Thresholding values in a grey image are selected by local adaptive strategy or man–machine interaction (Toure et al. 2019). Here, we have used the man–machine interaction method adopted to select the appropriate transect zone (T). Once the transition zone is derived, it is now implemented to the Landsat image to obtain a proper binary image. Land/water mask is applied to the image to separate into two classes. The image is segmented into two

groups of pixels: water (low values) group consisting of all pixels with grey level values < transition zone (T) and land (higher values) group consisting of pixels with values ≥ transition zone (T). The values below the transition zone (*T*) (representing water) are assigned as "1", and all the values above the *T* (representing land) are assigned as "0". Now, a binary image has been obtained. This image is named as a "processed image 1". Figure 4a represents the binary image of the histogram thresholding process.

The next step is to apply the band ratio technique to the grey images. This can be achieved by considering two separate spectral bands. Thao et al. (2008) have adopted the band ratio technique (band 2 — green/band 5 — mid-infrared) on Landsat ETM + image to extract the shoreline position. According to Tran and Trinh (2009), the band ratio method can reduce environmental induced variations. In the present study, band 2 and band 5 were considered for the band ratio technique. Once the band ratio (band 2/band 5) was performed, the output image is segmented into two classes, as shown in Fig. 4b. The image thus obtained from the band ratio technique is labels as 1 to all water pixels and 0 to all land pixels. Now, this binary image is named as a "processed image 2".

The images thus obtained through histogram thresholding (processed image 1) and band ratio technique (processed image 2) are then multiplied from one another. Multiplication of two images is carried out using the band math method in ENVI 5.3 V. This will create another binary image, as shown in Fig. 4c. The output images (binary image) are taken into the GIS environment, where the spatial analysis technique was adopted to convert the raster image to a vector file, which is zigzag in nature. Then, the smoothing operation was carried out to convert the zigzag line into a smooth line. Smoothing application in GIS is a generalization operation that removes the visual quality points from the line (ESRI, 1996). In the present study, the smoothing tolerance of 20 units was used. The smoothing operation was performed to convert the zigzag polyline into a smooth polyline in ArcGIS 10.3 V. The final polyline after smoothing represents the automated extracted shoreline position using the Landsat image.

Shoreline extraction using Resourcesat-2 (LISS-IV) image

The unsupervised classification (ISODATA) technique was applied to the Resourcesat-2 (LISS-IV) image. Here, the

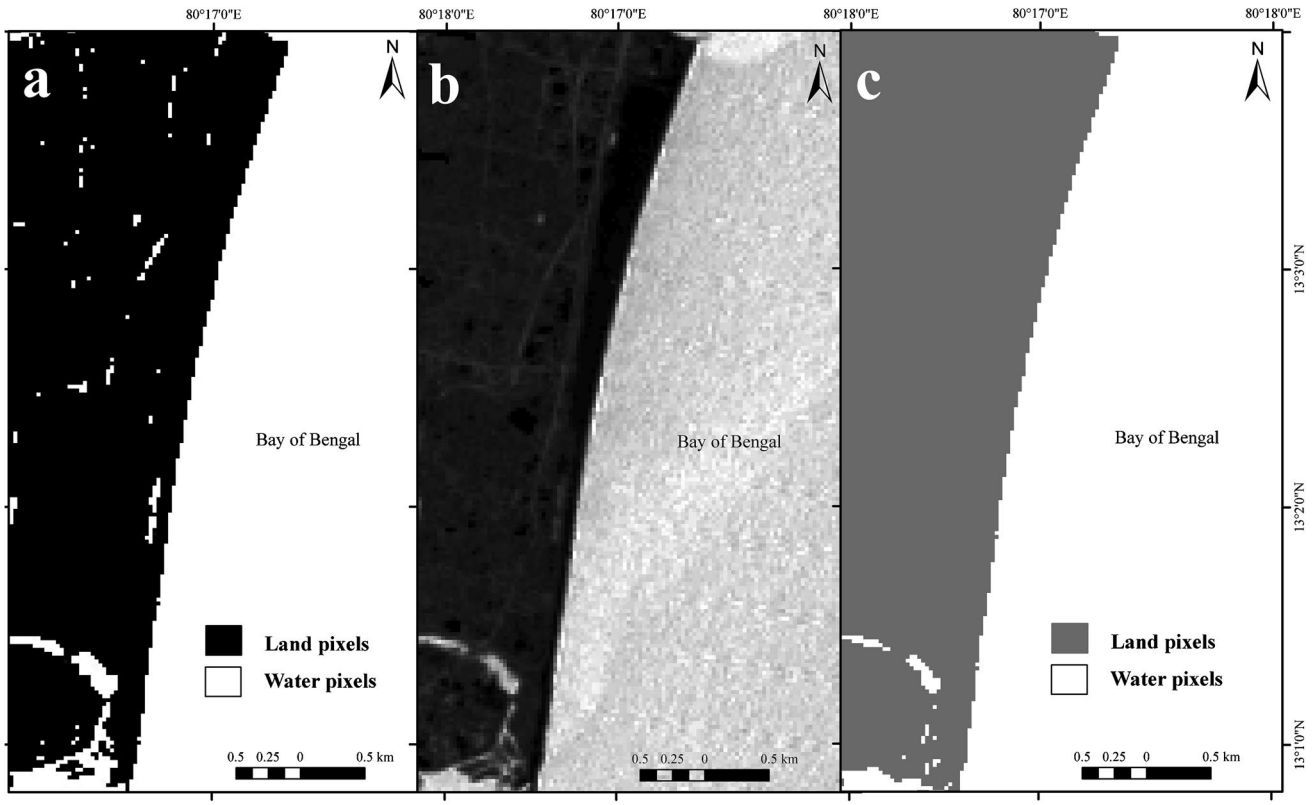

Fig. 4 **a** Binary image by histogram thresholding method of near-infrared band in Landsat image; **b** output image derived from band ratio technique (band 2/band 5) on Landsat image; **c** composite image derived from the multiplication of histogram thresholding method and band ratio technique

multi-spectral (green, red and infrared) bands were used for shoreline extraction. Each band has its unique characteristics in the land feature identification. The histograms of all three different bands are shown in Fig. 3b. Single-band itself is more suitable for ISODATA classification in shoreline extraction. However, to extract the shoreline position accurately, all three different bands were used together. ERDAS IMAGINE 2014 software was used to process the data.

Initially, the median filtering technique method was applied to the LISS-IV satellite image to reduce the noises present in the image. The median filtering technique is applied to an image to suppress specific frequencies and to emphasize others. According to Toure et al. (2019), filtering techniques are used for shoreline recognition and reduce the image noises. It even maintains the edge information of an image in a better way. In this technique, the pixel value of an image will be replaced with the median values. The replacement depends on the kernel or window size, which is applied to the image. In the present study, a 3×3 window is used to arrive at a median value of an image. This pre-processed filtered image is then used for the ISODATA classification technique.

Before the analysis, the threshold values for clustering and processing options need to be addressed based on the user's requirement. The clustering options include minimum and maximum clustering classes, minimum cluster size in pixel and minimum pixel distance. The processing option includes the number of iterations (run). The study area consists of different types of land features, and hence, the region is classified into 10 different classes. As mentioned earlier, Liu et al. (2011) have explained the need for a higher number of classifications for the coastal region. The number of iterations specified will determine the classification of the pixels into different cluster mean values. Therefore, each run will re-classify the mean cluster values until the maximum number is reached, and there is no further relocation of a pixel from one cluster to another. In the present study, the iteration value is set to 12. In a multi-spectral image, the minimum cluster size should be more than 10 times the bands used to obtain a dependable measurement (Liu et al. 2011). The pixel distance is the interval between row and column for each pixel, which is being sampled. If the Euclidean distance is less than the mentioned value, it will be merged to form a single cluster. Computation time will be reduced if the interval between the samples is large. However, it introduces a new bias factor in the statistics. The higher sample interval will reduce the time duration and reduce the accuracy in the output (Liu et al. 2011). Therefore, in this study, the minimum distance between the pixels is maintained to two.

Once all the required parameters were set, the ISODATA classification was applied to the LISS-IV image. The output image will be a clustered image of 15 different classes, as shown in Fig. 5a. Each cluster represents different land covers with similar pixel values clubbed together into particular clusters. Now, each cluster was represented in different colours for easy interpretation. The integer values of each pixel in a classified ISODATA image are shown in Table 2. A total of 834,678 pixels were classified into different classes. Class-2 (Ocean-mid) has the highest number of pixels (197,236), followed by class-1 (Ocean-open) with 179,481-pixel counts. The classification technique distinguishes the water body into different intensities, a typical phenomenon in our study. Figure 5a clearly shows different classes of water regions. Even though the entire ocean in our study represents shallow depth, the ocean region is categorized into different class names for understanding purposes. Out of 15 classes, 5 classes (ocean-open, ocean-mid, ocean-shallow, ocean-very shallow and breaker zone region) were assigned to ocean pixels. Classes 1, 2, 3, 4, 5, 10 and 14 are related to water pixels with different signatures. At the same time, the remaining classes represent different land features. Classes 14 and 15 show the sandy beach (dry) and (wet), respectively. Classes 6, 7, 8, 9, 11, 12 and 13 are related to land features, which are not related to the present study. Hence, these classes were omitted from the analysis and grouped as unclassified classes.

Visual interpretation of similar pixel values from the land and water was carried out for the entire scene to cluster the image. It was noticed that the pixel value of water is similar to the far-away object from the landside. For example, the road and other dark objects on the landside have similar pixel intensity of the water body. Hence, it is necessary to visualize the outcome to determine the misclassification pixels. In our classification, similar-intensity values are located far away, and there is no such pixel mismatch near the shoreline vicinity. These similar pixel values are grouped under the unclassified category. Classes 14 and 15 are of prime importance to our study, since the shoreline extraction is a proxy-based method. According to the shoreline definition, class 14 (sandy beach-wet) acts as a transition zone (Fig. 5b) between land/water boundaries. Once the classes were assigned, the image-recoding technique was adopted on the classified ISODATA image to create a classified image (land and water pixel). Therefore, classes 1, 2, 3, 4, 5, 10 and 14 were grouped into a single cluster (water class) and class 15 as a separate cluster (land with dry sandy beach). All other classes were clustered together as an unclassified class, as shown in Fig. 6. Now, these three groups were further recoded into two categories as land and water. Finally, the recoded water class contains 566,080-pixel numbers and the land class with 268,598 pixels. This recoded image will be the classified image used for shoreline extraction.

A land/water mask is applied to the classified image to separate the image into two classes. After the land mask, the image is separated into two-pixel groups. Water pixel values were assigned as 1, and land pixels were assigned as

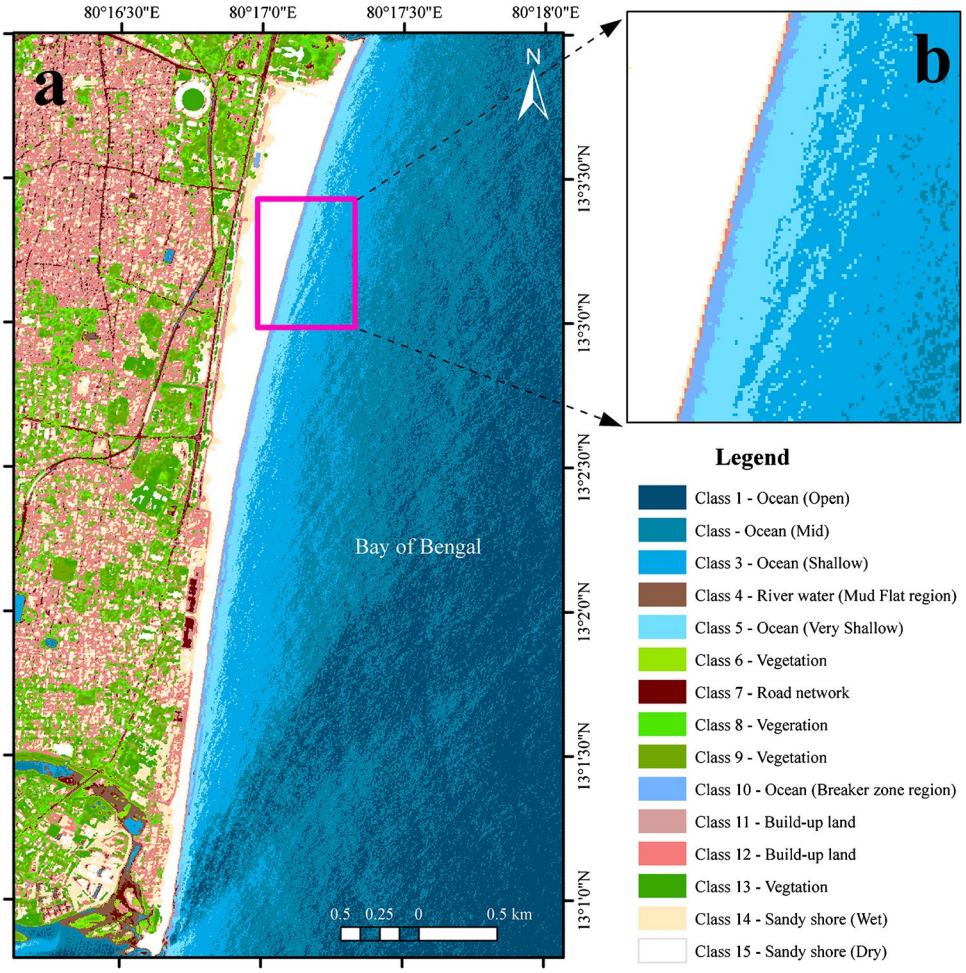

Fig. 5 **a** Clustered image with 15 different classes obtained by ISODATA classification method on LISS-IV image; **b** transition zone between sandy dry and wet beach for shoreline extraction

Table 2 Details of pixel values for each class obtained from ISODATA classification method

Pixel count	Classes	Name of the classes
179,481	Class 1	Ocean (open)
197,236	Class 2	Ocean (mid)
85,585	Class 3	Ocean (shallow)
8640	Class 4	River water (mud flat region)
22,777	Class 5	Ocean (very shallow)
11,995	Class 6	Vegetation
14,503	Class 7	Road network
31,710	Class 8	Vegetation
36,208	Class 9	Vegetation
5921	Class 10	Ocean (breaker zone region)
37,732	Class 11	Build-up land
72,927	Class 12	Build-up land
16,178	Class 13	Vegetation
66,440	Class 14	Sandy shore (wet)
47,345	Class 15	Sandy shore (dry)

0. Finally, a binary image has been obtained (Fig. 7). This binary image is then converted into vector format in ARC-GIS -10.3 V environment. A polyline feature obtained from the conversion process illustrates a zigzag line. A smoothing operation (smoothing tolerance of 20 units) was performed to convert the zigzag polyline into a smooth polyline. The line feature obtained after the smoothing process will represent the automated extracted shoreline position from Resourcesat-2 (LISS-IV) image.

Discussion

In present days, the emergence of remote sensing data (satellite data) has become a successful tool for various land and coastal applications. The spectral resolution of the satellite images will determine the shoreline approach, which needs to be adopted on any given coast. Even though there is a broad increase in spatial and spectral resolution of satellite data, the availability and cost of the data have been among the significant concerning factors for research work. Landsat satellite image is often considered for many spatial

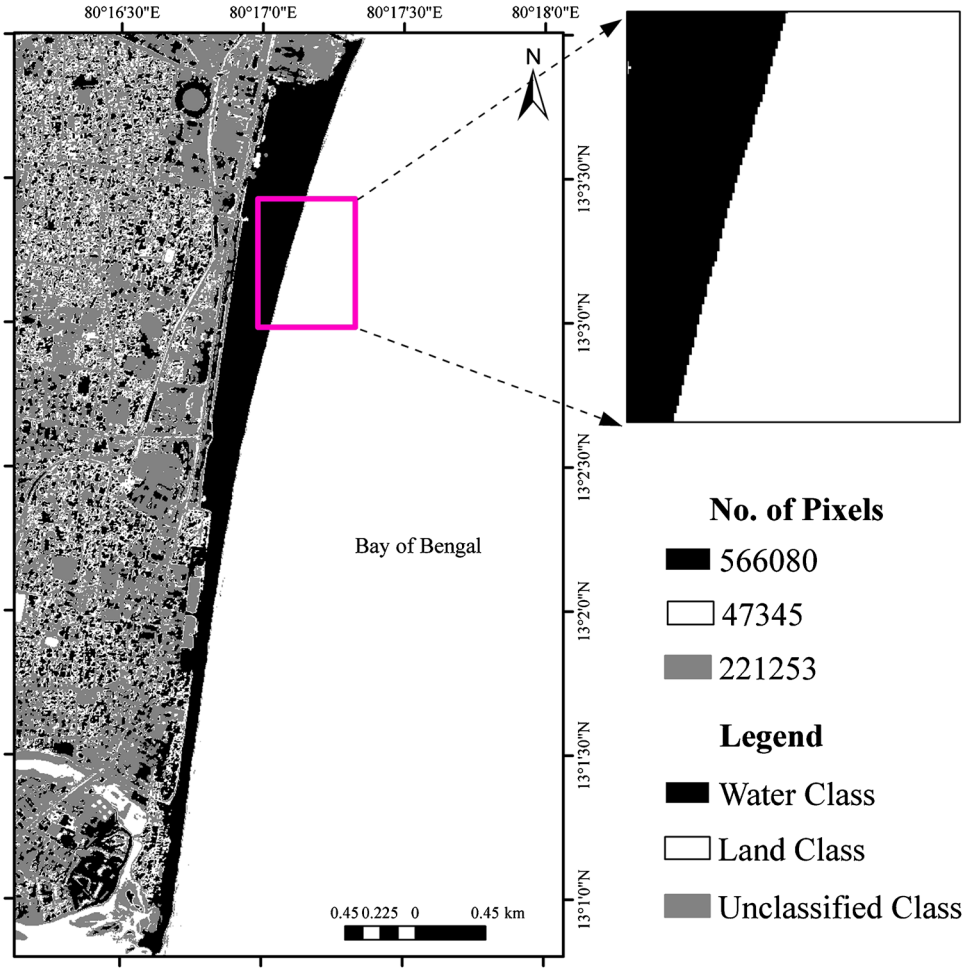

Fig. 6 Re-coding of ISODATA classified image into three classes

applications due to its free availability (USGS) and comprehensive aerial coverage. Automated shoreline extraction and its accuracy depend on the spatial resolution of the satellite image, which is being used. Therefore, the Landsat image was considered for automated shoreline extraction. Similarly, SPOT satellite images are too considered for shoreline change studies due to wide range of aerial coverage. However, the satellite data with high-resolution images are used very rarely due to the high cost of the data product. Most of the coastal researchers commonly prefer to publish their research article, which are related to medium-resolution satellite images, which are easily available with wide range of aerial coverage. In the past, many researchers have used Landsat images for shoreline extraction using different image processing techniques. However, due to the dynamic nature of shoreline positions, the question arises mainly on the limitations and accuracy of the outcome results. We have attempted to provide the best suitable method for automated shoreline extraction using image-processing techniques for medium-resolution satellite images (Landsat image). Similarly, an attempt was made even to high-resolution images to extract the shoreline positions. The results provide the best possible results for both high- and medium-resolution satellite images with the highest accuracy possible. The composite technique method adopted for Landsat (ETM+) image can be utilized for any different location in the world (coast being a sandy type) due to its free availability and wide range of aerial coverage. According to Guariglia et al. (2006), the ISODATA method has significant benefits in shoreline classification, particularly based on proxy (wet/dry) methods. As discussed earlier, the shoreline has different proxies, and therefore, performing a similar methodology for all the proxies does not yield appropriate results. In our study, there are still some limitations in the present methodology.

There are different digital image-processing techniques adopted by many researchers according to the specific study. The methods such as simple thresholding, band-ratio, NDWI, supervised and unsupervised classification techniques are used by the researchers for shoreline extraction. Each method has its own uniqueness and provides the output according to the interpreter requirements. The geomorphological condition of the coastal settings may determine the methods adopted for the particular study. In the present

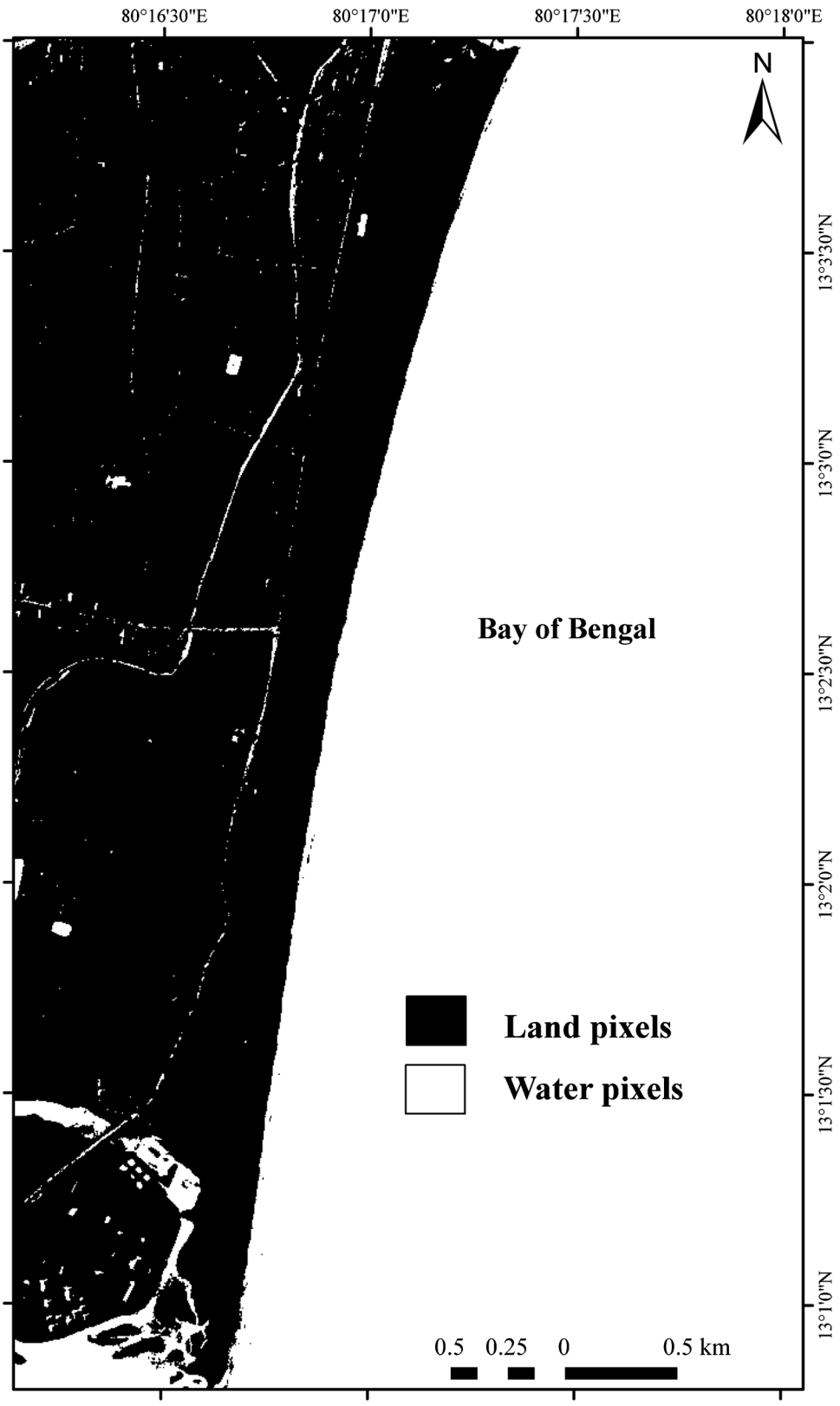

Fig. 7 The classified binary image of Resourcesat-2 satellite image

study, the single-band (grey scale) method was adopted on Landsat-7 and multi-spectral bands (green, red and near-infrared) on Resourcesat-2 image to extract the shoreline. In the electromagnetic spectrum, the near-infrared and mid-infrared band shows high absorption characteristics by water body. Due to this, the reflectance of water bodies will

be zero, whereas the land features show high reflectance in these wavelengths. According to Kelley et al. (1998), band 5 mid-infrared is considered as the best band for extracting the land–water boundary. Shoreline extraction from Landsat-7 image includes a composite technique of histogram thresholding and band ratio technique. Initially, the histogram thresholding method was implemented on the near-infrared band of the Landsat-7 image, which is named as processed image 1. Band ratio was adopted between green (band 2) and mid-infrared (band 5) images and named as a processed image 2. Finally, band multiplication was carried out by multiplying the processed images 1 and 2. In this process, a new binary image (raster image) is obtained which is converted into a vector format in ArcGIS environment. Like this, the shoreline position is obtained from the Landsat image. Similarly, the shoreline position from LISS-IV image was obtained using multi-spectral bands. Here, the median filtering technique was performed on multi-spectral bands (green, red and near-infrared) of the Resourcesat-2 (LISS-IV) image. ISODATA technique was applied to the multi-spectral filtered image to classify into different classes. Then, re-coding of different classes in to land, water and unclassified-mixed pixels was carried out. Finally, the re-coded image is classified into land and water pixels separately based on the shoreline proxy (wet/dry line).

The accuracy assessment of the Landsat-7 image (medium-resolution) could not be carried out due to the non-availability of field data at that particular time. The field survey was undertaken on 6 April 2013. However, the acquired Landsat image has a 2-week difference. Hence, comparing the extracted shoreline from the Landsat image with a field survey will not be appropriate. However, when compared to the LISS-IV shoreline, the shoreline extracted from the Landsat image shows less than a pixel accuracy. Shoreline validation and accuracy assessment were carried out by quantitative evaluation method. In quantitative method, validation of shoreline is carried out by comparing the field-measured shoreline position with the extracted shoreline from the fixed baseline. The normalized difference water index (NDWI), supervised classification (ML) method and K-mean method were compared with the ISODATA method. Each method has its own uniqueness for shoreline extraction. Table 3 shows the comparison of all the classifications techniques. The differences in each method were within the pixel limit. However, ISODATA method shows more accuracy while comparing with other methods. The outcome of ISODATA methods, particularly water body mapping, shows an accuracy of more than 95% (Kuleli 2010). The methodology adopted in our study is applicable primarily where the shore represents the sandy coast. Moreover, the accuracy of the shoreline detection method depends on the interpreter's knowledge. According to Mitra et al. (2017), the type of coast (wave-dominated, tide-dominated and mixed) also influences the results. The accuracy of shoreline positions depends on selecting appropriate thresholding values (Aktas et al. 2012). There is no standalone method to extract the shoreline position from satellite images with 100% accuracy. According to Toure et al. (2019), the spatial resolution of an image determines the shoreline extraction method. Therefore, understanding the coast is very important for extracting the coastal features. In manual methods, it required an expert to interpret the shoreline positions, which sometimes may lead to misinterpretation of the shoreline positions. However, the pixel-based classification technique will provide a comprehensive, reliable and repetitive method for shoreline extraction from optical satellite images, which a non-expert can run.

Accuracy assessment

The shoreline positions obtained from satellite images need to be validated with the in situ data. Mitra et al. (2017) have elucidated several methods to estimate accuracies, such as comparing with Google earth image (high resolution), field-collected GCP and raw image. However, each method of comparison has its merit and demerit. For example, the Google earth image cannot be compared with the medium-resolution satellite image. Moreover, the image acquisition period is different from one another. Garcia-Rubio et al. (2014) have validated the extracted shoreline with the field measurement. In the present study, in situ measurements were used to compare the shoreline positions. In the field survey method, the constraint of the coast can be interpreted in a better way (Selvan et al. 2020). For precise accuracy assessment, the shoreline extracted from Resourcesat-2 image is considered for comparison. Initially, shorelines were tracked for the entire study site using a handheld GPS (Trimble GEO XH 6000) instrument. This handheld GPS (Trimble GEO XH 6000) has an accuracy of 1–3 m.

The repeatability period of the Resourcesat-2 satellite was marked earlier, and then the field survey measurement was planned accordingly. The entire stretch of 6 km was tracked with the handheld GPS. The shoreline position tracking started precisely 1 h before the satellite pass and was completed 1 h later. Hence, it took 3 h to complete the field measurement for the entire coastal stretch. The shoreline extracted from satellite imagery is then compared with the field-collected in situ shoreline data. The method adopted is similar to that of shoreline analysis in DSAS software. Initially, a baseline was created on the landward side of the shorelines, which act as a starting point of all transects. Then, transects were generated from the baseline, which intersect on both the shoreline positions. These transects will intersect the shorelines at every 250 m and calculate the distance from the fixed baseline position. A total of 24 transects

Table 3 Differences between the shorelines (measured and extracted shorelines) at each transect positions for ISODATA, K-mean, maximum likelihood and NDWI methods

Transects	Shoreline — ISODATA method (distance from baseline)				Field measured shoreline (distance from baseline)	Differences			
	ISODATA	K-mean	Maximum likelihood	NDWI		ISODATA	K-mean	Maximum likelihood	NDWI
1	24.90	26.8	26.5	26.07	25.55	0.65	1.25	0.95	0.52
2	28.06	28.41	28.61	28.73	26.11	1.95	2.3	2.5	2.62
3	33.26	32.77	32.36	31.96	28.86	4.41	3.91	3.5	3.1
4	32.20	32.62	32.79	32.41	30.97	1.23	1.65	1.82	1.44
5	32.30	32.79	32.39	32.95	31.98	0.33	0.81	0.41	0.97
6	35.70	35.77	36.34	36.65	33.82	1.88	1.95	2.52	2.83
7	31.02	32.32	32.59	32.91	31.49	0.48	0.83	1.1	1.42
8	35.52	35.72	35.22	36.09	32.70	2.81	3.02	2.52	3.39
9	36.43	36.7	36.25	36.78	35.05	1.38	1.65	1.2	1.73
10	32.79	34.59	35.25	35.14	33.89	1.10	0.7	1.36	1.25
11	34.47	34.74	34.99	35.33	33.51	0.96	1.23	1.48	1.82
12	36.09	36.49	36.81	36.99	35.87	0.22	0.62	0.94	1.12
13	32.60	32.95	32.7	32.85	32.11	0.49	0.84	0.59	0.74
14	36.69	37.89	37.7	38.09	36.99	0.30	0.9	0.71	1.1
15	37.54	38.09	38.36	37.88	36.35	1.19	1.74	2.01	1.53
16	33.72	36.14	36.42	35.76	34.82	1.10	1.32	1.6	0.94
17	35.69	40.14	39.59	39.67	37.74	2.05	2.4	1.85	1.93
18	37.32	37.72	37.8	37.59	36.02	1.30	1.7	1.78	1.57
19	40.07	40.7	40.83	41.35	38.75	1.32	1.95	2.08	2.6
20	36.74	37.09	37.33	37.61	36.81	0.07	0.28	0.52	0.8
21	36.99	38.61	38.44	38.32	37.60	0.62	1.01	0.84	0.72
22	36.07	36.54	36.32	36.62	36.12	0.06	0.42	0.2	0.5
23	34.96	35.55	35.9	35.7	34.60	0.36	0.95	1.3	1.1
24	37.21	39.1	38.6	38.9	38.00	0.79	1.1	0.6	0.9

were generated to validate the shoreline position (Fig. 8a). The graph in Fig. 8b clearly shows that differences between the shorelines (measured and extracted shorelines) at each transect were within the limit of a pixel value of LISS-IV (5.8 m) data. Of the values, 87.5% were < 2 m accuracy, and only 3 transects, which account for 12%, is more than 2 m but within a pixel limit (Table 3).

Comparison between different classification techniques

Satellite-derived shorelines from different classification techniques (ISODATA, NDWI, ML and K-mean) were validated with field-measured shoreline positions. A quantitative evaluation method was applied to compare the shoreline positions. A standard fixed baseline (reference line) was drawn from where the satellite-derived shorelines are compared with one another. A total of 24 transects were generated from baseline which intersect all the shoreline positions. All the transects were generated perpendicular to the shoreline positions. In comparison to different shoreline positions with respect to baseline, it is clear that the comparison values obtained from ISODATA method are much closer to the field values than others. The other methods (NDWI, ML and K-mean) provide a reasonable result; the ISODATA method emerged as a promising method for shoreline extraction automatically. Table 3 shows the comparison of all the four different methods. In ISODATA method, of 87.5% transects was less than 2 m accuracy, whereas the K-mean method shows 83% which is closer to ISODATA method. However, the other methods such as NDWI and maximum likelihood show the accuracy of 79% and 75%, respectively. The comparison clearly shows that the ISODATA method gives a good correlation and hence proves to be the better method for shoreline extraction automatically. Guariglia et al. (2006) have stated that the ISODATA classification method has higher supremacy over other methods when interpreting the proxy-based shoreline such as wet/dry line and other features such as dunes and vegetation. Similarly, Zhang (2000) has suggested that the

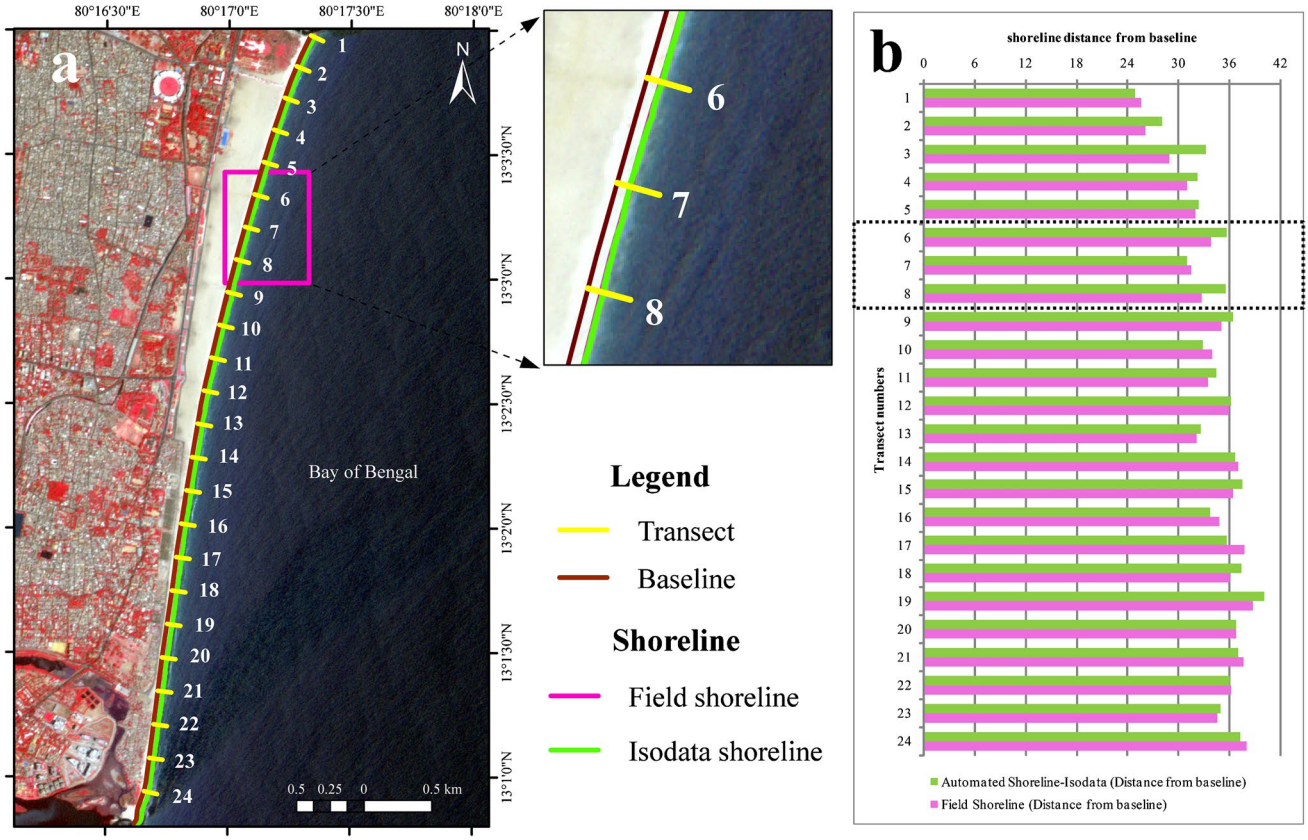

Fig. 8 **a** Transect intersection between field-measured shoreline with satellite-derived shoreline for comparison and validation; **b** the graph showing the differences between the shorelines (measured and extracted shorelines) at each transects positions

ISODATA method has shown prominent results even when the water body has higher mixed pixels values.

Conclusion

A pixel-based classification technique was developed to automatically extract the proxy-based (wet/dry) shoreline positions from optical satellite images. Two approaches were developed to identify the proxy-based shoreline position from optical satellite images. A pixel-based composite technique, a combination of band ratio and thresholding, was implemented on the Landsat-7 (ETM +, medium-resolution) image. The ISODATA classification technique was applied to Resourcesat-2 (LISS-IV, high-resolution) image. The outcome from the analysis indicates that the proposed methodology is more competent and provides a comprehensive, reliable and repetitive method for shoreline extraction from optical satellite images. Moreover, it reduces the cost and limits the time duration for shoreline extraction with accuracy. The methods adopted in the present study can be utilized on any different coast, provided if the shoreline proxy is sandy. Instead, a similar application cannot be used on other types of shoreline proxies. Satellite-derived shorelines from different classification techniques (ISODATA, NDWI, ML and K-mean) were validated with field-measured shoreline positions. The extracted shoreline from Resourcesat-2 (LISS-IV) satellite image at each transect was well-matched with the field-measured (handheld GPS) shoreline, and the values are found to be within the pixel limit (LISS-IV 5.8 m), and 87.5% of the values have < 2 m accuracy. The K-mean, NDWI and maximum likelihood methods show the accuracy of 83%, 79% and 75% respectively. The automatic extraction of shoreline using image-processing techniques will enhance the visibility of ground features and reduce the possible manual errors, as it is a replicable technique adopted on any sandy coast.

Acknowledgements We sincerely thank the Secretary, Ministry of Earth Sciences (MoES), Government of India (GoI) and the Director, National Centre for Coastal Research (NCCR) and project stuffs for their kind support and valuable suggestions for this work.

Author contribution Dr. S. Chenthamil Selvan: original manuscript preparation, methodology preparation, data analysis, interpretation and field investigation. Dr. R. S. Kankara: conceptualization, data

interpretation, correction and finalizing Manuscript. MR. Prabhu K: involved in testing and maps creation, field investigation.

Funding Present study is a part of research work being carried out in National Centre for Coastal Research (NCCR), Ministry of Earth Sciences (MoES).

Data availability The data source of each satellite images used is mentioned in the manuscript.

Code availability Not applicable.

Declarations

Ethics approval The authors confirm that the study was approved by the National Centre for Coastal Research (NCCR), which is a nodal institute.

Consent to participate Not applicable.

Consent for publication Not applicable.

Conflict of interest The authors declare that they have no competing interests.

References

Abdelhady HU, Cary T, Ayman H, Raja M (2022) A simple, fully automated shoreline detection algorithm for high-resolution multispectral imagery. Remote Sens 14(3):557. https://doi.org/10.3390/rs14030557

Aedla R, Dwarakish GS, Reddy DV (2015) Automatic shoreline detection and change detection analysis of Netravati-Gurpur River mouth using histogram equalization and adaptive thresholding techniques. Aquat Procedia 4:563–570. https://doi.org/10.1016/j.aqpro.2015.02.073

A'Kif AF, Lawal B, Pradhan B (2011) Semi-automated procedures for shoreline extraction using single Radarsat-1 SAR image. Estuar Coast Shelf Sci 95(4):395–400. https://doi.org/10.1016/j.ecss.2011.10.009

Aktas UR, Can G, Vural FTY (2012) A robust approach for shoreline detection in satellite imagery. 20th Signal Process Commun Appl Conf (SIU), Mugla. 1–4. doi: https://doi.org/10.1109/SIU.2012.6204797

Al Mansoori S, Al Mansoori S, Al Marzouqi F (2016) Coastline extraction using satellite imagery and image processing techniques. Int J Curr Eng Technol 6(4):1245–1251

Alesheikh AA, Ghorbanali A, Nouri N (2007) Coastline change detection using remote sensing. Int J Environ Sci Technol 4:61–66. https://doi.org/10.1007/BF03325962

Apostolopoulos D, Nikolakopoulos K (2021) A review and meta-analysis of remote sensing data, GIS methods, materials and indices used for monitoring the coastline evolution over the last twenty years. Eur J Remote Sens 54(1):240–265. https://doi.org/10.1080/22797254.2021.1904293

Biswajeet P, Rizeei HM, Abdulle A (2018) Quantitative assessment for detection and monitoring of coastline dynamics with temporal RADARSAT images. Remote Sens 10(11):1705. https://doi.org/10.3390/rs10111705

Boak E, Turner I (2005) Shoreline definition and detection: a review. J Coast Res 21:688–703. https://doi.org/10.2112/03-0071.1

Braud DH, Feng W (1998) Semi-automated construction of the Louisiana coastline digital land/water boundary using Landsat Thematic Mapper satellite imagery. Louisiana Applied Oil Spill Research and Development Program, OS2 RAPD Technical Report Series 97(002)

Chang CI, Brumbley C (1999) A Kalman filtering approach to multispectral image classification and detection of changes in signature abundance. IEEE Trans Geosci Remote Sens 37(1):257–268. https://doi.org/10.1109/36.739160

Chen Chao Fu, Jiaoqi ZS, Xin Z (2019) Coastline information extraction based on the tasseled cap transformation of Landsat-8 OLI images. Estuar Coast Shelf Sci 217:281–291. https://doi.org/10.1016/j.ecss.2018.10.021

DeWitt H, Weiwen Feng JR (2002) Semi-automated construction of the Louisiana coastline digital land-water boundary using Landsat TM imagery. Louisiana State University Louisiana's Oil Spill Research and Development Program, Baton Rouge, p 70803

Di K, Wang J, Ma R, Li R (2003) Automatic shoreline extraction from high-resolution IKONOS satellite imagery. ASPRS Annual Conference Proceedings, Anchorage, Alaska. 3

Ellis JM, Caldwell PO, Goodwin PB (1991) Merging satellite images and maps to improve operations: Niger Delta, Nigeria. Conference: Annual meeting of the American Association of Petroleum Geologists (AAPG) Dallas 75(3):568–569

ESRI (1996) Automation of map generalization - the cutting-edge technology. ESRI, United States of America

Fenster MS, Dolan R (1999) Mapping erosion hazard areas in the city of Virginia Beach. J Coast Res SI 28:58–68

Fisher JS, Overton MF (1994) Interpretation of shoreline position from aerial photographs. Int Conf Coastal Eng 1(24). Doi: https://doi.org/10.9753/icce.v24.%p

Fletcher CH, Rooney JJB, Barbee M, Lim SC, Richmond BM (2003) Mapping shoreline change using digital ortho photogrammetry on Maui. Hawaii J Coast Res SI 38:106–124

Frazier PS, Page KJ (2000) Water body detection and delineation with Landsat TM data. Photogramm Eng Remote Sens 66(12):147–167

Garcia-Rubio G, Huntley D, Russell P (2014) Evaluating shoreline identification using optical satellite images. Mar Geol 359:96–105. https://doi.org/10.1016/j.margeo.2014.11.002

Guariglia A, Buonamassa A, Losurdo A, Saladino R, Trivigno ML, Zaccagnino A, Colangelo AC (2006) A multisource approach for coastline mapping and identification of shoreline changes. Ann Geophys 49(1). https://doi.org/10.4401/ag-3155

Hapke CJ, Reid D (2007) National assessment of shoreline change, part 4: historical coastal cliff retreat along the California Coast. US Geological Survey, Reston, VA, USA, Open-file Report 2007–1133

Hinkel J, Lincke D, Vafeidis AT, Perrette M, Nicholls RJ, Tol RSJ, Marzeion B, Fettweis X, Ionescu C, Levermann A (2014) Coastal flood damage and adaptation cost under 21st century sea-level rise. Proc Natl Acad Sci 111(9):3292–3297. https://doi.org/10.1073/pnas.1222469111

Hoeke RK, Zarillo GA, Synder M (2001) A GIS based tool for extracting shoreline positions from aerial imagery (BeachTools). Coastal and Hydraulics Engineering Technical Note CHETN-IV-37, U.S. Army Engineer Research and Development Center, Vicksburg, MS. http://chl.wes.army.mil/library/publications/chetn/

Hwang DJ (1981) Beach changes on Oahu as revealed by aerial photographs. Hawaii Office of State Planning Coastal Zone Management Program, Honolulu, p 146

Jishuang Q, Chao W (2002) A multi-threshold based morphological approach for extraction coastal line feature in remote sensed images. Pecora 15/L & Satellite Information IV Conference (Denver, Colorado), ISPRS Commission I/FIEOS, 319–338. Retrieved from http://www.wins.uva.nl/research/isis

Kankara RS, Murthy M, Rajeevan M 2018 National assessment of shoreline changes along Indian Coast: Status report for 26 years (1990 - 2016)

Kelley John GW, Hobgood JS, Bedford KW, Schwab DJ (1998) Generation of three-dimensional lake model forecasts for Lake Erie. J Weather Forecast 13(3):659–687. https://doi.org/10.1175/1520-0434(1998)013%3c0659:GOTDLM%3e2.0.CO;2

Kingsford RT, Thomas RF, Wong PS, Knowels (1997) GIS database for wetlands of the Murray Darling basin. Final report to the Murray-Darling Basin Commission, National parks and wildlife service, Sydney, Australia, 85

Krishna GM, Mitra D, Ak M, Oyuntuya Sh, Nageswara Rao K (2005) Evaluation of semi-automated image processing techniques for the identification and delineation of coastal edge using IRS, LISS-III image - a case study on Sagar Island, east coast of India. Int J Geoinformatics 1:67–76

Kuleli T (2010) Quantitative analysis of shoreline changes at the Mediterranean coast in Turkey. Environ Monit Assess 167:387–397. https://doi.org/10.1007/s10661-009-1057-8

Lillesand TM, Kiefer RW, Chipman AW (2015) Remote sensing and image interpretation, 7th edn. Wiley, New York

Liu H, Jezek KC (2004) Automatic extraction of coastline from satellite imagery by integrating canny edge detection and locally adaptive thresholding methods. Int J Remote Sens 25(5):937–958. https://doi.org/10.1080/0143116031000139890

Liu H, Wang L, Sherman DJ, Wu Q, Su H (2011) Algorithmic foundation and software tools for extracting shoreline features from remote sensing imagery and LiDAR data. J Geogr Inf Syst 3:99–119. https://doi.org/10.4236/jgis.2011.32007

Luijendijk A, Hagenaars G, Ranasinghe R, Baart F, Donchyts G, Aarninkhof S (2018) The state of the world's beaches. Sci Rep 8:6641. https://doi.org/10.1038/s41598-018-24630-6

Mentaschi L, Vousdoukas MI, Pekel J-F, Voukouvalas E, Feyen L (2018) Global long-term observations of coastal erosion and accretion. Sci Rep 8:12876. https://doi.org/10.1038/s41598-018-30904-w

Mitra SS, Mitra D, Santra A (2017) Performance testing of selected automated coastline detection techniques applied on multispectral satellite imageries. Earth Sci Inform 10:321–330. https://doi.org/10.1007/s12145-017-0289-3

Moore LJ (2000) Shoreline mapping techniques. J of Coast Res 16(1):111–124

Moore LJ, Griggs GB (2002) Long-term cliff retreat and erosion hotspots along the central shores of the Monterey Bay National Marine Sanctuary. Mar Geol 181(1–3):265–284. https://doi.org/10.1016/S0025-3227(01)00271-7

Moore LJ, Ruggiero P, List JH (2006) Comparing mean high water and high water shorelines: should proxy-datum offsets be incorporated into shoreline change analysis? J Coast Res 22(4):894–905. https://doi.org/10.2112/04-0401.1

Morton RA, Miller TL, Moore LJ (2004) National assessment of shoreline change: Part 1, historical shoreline changes and associated coastal land loss along the U.S. Gulf of Mexico, U.S. Geological Survey Open File Report 2004–1043, 44

Nayak SR (2002) Use of satellite data in coastal mapping. Indian Cartogr 22:147–157

Norcross ZM, Fletcher CH, Merrifield M (2002) Annual inter-annual changes on a reef-fringed pocket beach: Kailua Bay. Hawaii Mar Geol 190:553–580. https://doi.org/10.1016/S0025-3227(02)00481-4

Otsu N (1979) A threshold selection method from grey scale histogram. IEEE Trans Syst Man Cybern 9(1):62–66. https://doi.org/10.1109/TSMC.1979.4310076

Overton MF, Grenier RR, Judge EK, Fisher JS (1999) Identification and analysis of coastal erosion hazard areas: Dare and Brunswick counties. North Carolina J Coast Res S I(28):69–84

Pais-Barbosa J, Teodoro A, Veloso-Gomes F, Taveira-Pinto F, Gonçalves H (2011) How can remote sensing data/techniques help us to understand beach hydromorphological behavior? Littoral 12002(2011):9. https://doi.org/10.1051/litt/201112002

Parker DC, Wolff MF (1965) Remote sensing. Int. Sci Technol 43:20–31

Rogers Martin SJ, Mike B, Sue B, Tom S (2021) VEdge_Detector: automated coastal vegetation edge detection using a convolutional neural network. Int J Remote Sens 42:4809–4839. https://doi.org/10.1080/01431161.2021.1897185

Sekovski I, Stecchi F, Mancini F, Del Rio L (2014) Image classification methods applied to shoreline extraction on very high-resolution multi-spectral imagery. Int J Remote Sens 35(10):3556–3578. https://doi.org/10.1080/01431161.2014.907939

Selvan SC, Kankara RS, Prabhu K, Rajan R (2020) Shoreline change along Kerala, south-west coast of India, using geo-spatial techniques and field measurement. Nat Hazards 100:17–38. https://doi.org/10.1007/s11069-019-03790-2

Shalowitz AL (1964) Shore and sea boundaries with special reference to the interpretation and use of Coast and Geodetic Survey Data (Publication 10–1). Washington, DC: US Government Printing Office, US Department of Commerce, Coast and Geodetic Survey.

Song Y, Liu F, Ling F, Yue L (2019) Automatic semi-global artificial shoreline subpixel localization algorithm for Landsat imagery. Remote Sens 11(15):1779. https://doi.org/10.3390/rs11151779

Stafford DB, Langfelder J (1971) Air photo survey of coastal erosion. Photogramm Eng 37(6):565–575

Stockdon HF, Sallenger AH, List JH, Holman RA (2002) Estimation of shoreline position and change using airborne topographic LIDAR data. J Coast Res 18(3):502–513

Tao Q, Lewis AJ, Braud DH (1993) Change detection using multi-temporal feature space with digital TM data. Proceedings of 1993 ACSM/ASPRS Annual Convention and Exposition, New Orleans, Lousiana, February 15–18, ASPRS, Bethesda, MD, 2:364–373

Tarmizi N, Samad AM, Yusop S (2014) Shoreline data extraction from QuickBird satellite image using semi-automatic technique. Proceedings - 2014 IEEE 10th International Colloquium on Signal Processing and Its Applications, CSPA. 157-162 https://doi.org/10.1109/CSPA.2014.6805739

Thao PTP, Duan HD, To DV (2008) Integrated remote sensing and GIS for calculating shoreline change in Phan-Thiet Coastal Area. In Proceedings of the International Symposium on Geoinformatics for Spatial Infrastructure Development in Earth and Allied Sciences, Hanoi, Vietnam, 4–6 December

Thieler ER, Himmelstoss EA, Zichichi JL, Ayhan E (2009) Digital shoreline analysis system (DSAS) version 4.0. An ArcGIS extension for calculating shoreline change. U.S. Geological Survey Open-File Report 2008:1278–1279 (**Http://pubs.usgs.gov/of/2008/1278/**)

Tittley B, Solomon SM, Bjerkelund C (1994) The integration of Landsat TM, SPOT, and ERS-1 C-Band SAR for coastal studies in the MacKenzie River Delta, NWT, Canada: A preliminary assessment. Proc Second Thematic Conference on Remote Sensing for Marine and Coastal Environments, New Orleans, LA, I.225-I.236

Toure S, Diop O, Kpalma K, Maiga AS (2019) Shoreline detection using optical remote sensing: a review. ISPRS Int J Geo-Inf 8(2):75. https://doi.org/10.3390/ijgi8020075

Tran TV, Trinh TB (2009) Application of remote sensing for shoreline change detection in Cuu long estuary. VNU J Sci Earth Sci 25(4):217–222 (https://js.vnu.edu.vn/EES/article/view/1879)

Xu H (2006) Modification of normalised difference water index (NDWI) to enhance open water features in remotely sensed imagery. Int J Remote Sens 27(14):3025–3033. https://doi.org/10.1080/01431160600589179

Yasir M, Sheng H, Fan H, Nazir S, Niang JA, Sulaiman K (2020) Automatic coastline extraction and changes analysis using remote

sensing and GIS technology. IEEE Access 8:180156–18070. https://doi.org/10.1109/ACCESS.2020.3027881

Zhang Y (2000) A method for continuous extraction of multi-spectrally classified urban rivers. Photogramm Eng Remote Sens 66(8):991–999

Zuzek PJ, Nairn RB, Thieme SJ (2002) Spatial and temporal considerations for calculating shoreline change rates in the Great Lakes basin. J Coast Res 38:125–146